Chaotic Modeling and Simulation (CMSIM) 3: 179–189, 2021

Bifurcation and Chaos in a Discrete Prey-Predator Model

Anuraj Singh[1] and Pradeep Malik[2]

[1] ABV-Indian Institute of Information Technology and Management Gwalior, M.P.,India
(E-mail: anuraj@iiitm.ac.in)
[2] SGT University, Gurugram, India
(E-mail: pradeepmaths@gmail.com)

Abstract. In this paper, a modified Leslie-Gower predator-prey discrete model with Michaelis-Menten type prey harvesting is investigated. It is shown that the model exhibits several bifurcations of codimension 1 viz. Neimark-Sacker bifurcation, transcritical bifurcation and flip bifurcation on varying one parameter. The extensive numerical simulation is performed to demonstrate the analytical findings. The system exhibits periodic solution including flip bifurcation, Neimark-Sacker bifurcation followed by the wide range of dense chaos. .

Keywords: Discrete model, Codimension 1, Flip bifurcation, Neimark-Sacker bifurcation.

1 Introduction

The resource-consumer species interaction is one of the most common and focal research area in the field of mathematical biology. The dynamics of population models is concerned with population size, age distribution and many other natural factors. In biological systems, there are a number of models in which time is taken as a continuous function [1–3]. For population model this could be seen as a overlapping situation which implies a continuous series of birth and death processes and these models are usually performed by ordinary differential equations.

The discrete time population models are pertinent for non-overlapping generation models [4–6] and thus seems to be more realistic than continuous one. Many researchers investigated discrete-time models and gave interesting dynamics of the system by exploring several type of bifurcations [7–11].

The Lotka-Volterra prey-predator model with discrete time was firstly introduced by Maynard Smith [12] and studied by Levine [13] and Liu and Xiao [14]. It has been shown that these discrete time models undergo several bifurcations such as fold bifurcation, flip bifurcation and Neimark-Sacker bifurcation.

Received: 6 July 2020 / Accepted: 18 July 2021

ISSN 2241-0503

Moreover, Hadelar and Gerstmann [15] were the first who derives a discrete time model involving Holling type-II functional response using continuous time model. Also the complete discussion for the bifurcations of codimension 1 and parametric restriction for non-hyperbolicity has been done by Li and Zhang [16]. In another study, the authors discussed the chaotic dynamics of a discrete prey-predator model with Holling type-II functional response [6]. Singh and Deolia investigated a discrete-time the prey-predator model with Leslie-Gower functional response [11]. In their study the system exhibited Neimark-Sacker bifurcation, flip bifurcation and fold bifurcation under certain conditions.

2 Mathematical Model

Aziz-Alaoui and Daher Okiye [17] proposed the following two-dimensional prey-predator model with modified version of Leslie-Gower and Holling type II functional response:

$$\begin{aligned}\frac{dx}{dt} &= \left(r_1 - b_1 x - \frac{a_1 y}{k_1 + x}\right) x \\ \frac{dy}{dt} &= \left(r_2 - \frac{a_2 y}{k_2 + x}\right) y \end{aligned} \tag{1}$$

with positive initial conditions $x(0) \geq 0$ and $y(0) \geq 0$, when $x(t)$ and $y(t)$ represent the population densities at time t. Here r_1 denotes growth rate of prey and b_1 represents strength of competition among individuals in prey. The parameter $k_1(k_2)$ signifies the extent of protection provided by environment to the prey (predator) and r_2 describes the growth rate of y. $a_1(a_2)$ measures the maximum value per capita reduction rate of prey x (predator y). All the parameters are assumed to be positive.
The model (1) with Michaelis-Menten type harvesting under the assumption that same extent ($k_1 = k_2 = k$) to which environment provided protection to both the predator and prey [18,19] is given by:

$$\begin{aligned}\frac{dx}{dt} &= \left(r_1 - b_1 x - \frac{a_1 y}{k + x}\right) x - \frac{cEx}{m_1 E + m_2 x} \\ \frac{dy}{dt} &= \left(r_2 - \frac{a_2 y}{k + x}\right) y \end{aligned} \tag{2}$$

Here c signifies catchability coefficient and E denotes harvesting effort in prey species. Where m_1 and m_2 are suitable constants. All the parameters are assumed to be positive and similar meaning as of (1).
To investigate the dynamics of the system (2), the following non-dimensional scheme is taken:

$$x = \frac{r_1 x}{b_1}, \quad t = \frac{t}{r_1}, \quad y = \frac{r_1^2 y}{a b_1^2}$$

$$p = \frac{1}{b_1}, \quad \alpha = \frac{cEb_1}{m_2 r_1^2}, \quad \gamma = \frac{b_1 k}{r_1}, \quad \delta = \frac{m_1 E b_1}{m_2 r_1}, \quad \beta = \frac{r_2}{r_1}, \quad q = \frac{a_2}{a_1 b_1}$$

Using the above scheme, we get the following non-dimensional system:

$$\begin{aligned}\frac{dx}{dt} &= x\left(1 - x - \frac{py}{\gamma + x} - \frac{\alpha}{\delta + x}\right)\\ \frac{dy}{dt} &= \beta y\left(1 - \frac{qy}{\gamma + x}\right)\end{aligned} \tag{3}$$

with the initial conditions $x(0) = x_0 \geq 0, \quad y(0) = y_0 \geq 0$.

Gupta and Chandra [20] investigated the continuous-time model (3) and determined several local bifurcations viz. Hopf bifurcation, saddle-node, transcritical bifurcation and Bogdanov-Takens bifurcation.
In order to derive discrete time model from the system (3) employing forward Euler scheme and taking ϵ is the step size. Letting $\epsilon \to 1$ then $(n+1)^{th}$ generation of the prey-predator population is governed by following set of equations:, it is obtained

$$\begin{aligned}x_{n+1} &= x_n + x_n\left(1 - x_n - \frac{py_n}{\gamma + x_n} - \frac{\alpha}{\delta + x_n}\right)\\ y_{n+1} &= y_n + \beta y_n\left(1 - \frac{qy_n}{\gamma + x_n}\right)\end{aligned} \tag{4}$$

with initial conditions $x(0) = x_0$, and $y(0) = y_0$.
Now, the discrete time prey-predator model can be defined by a mapping

$$G : \begin{pmatrix} x \\ y \end{pmatrix} \to \begin{pmatrix} x + x\left(1 - x - \frac{py}{\gamma+x} - \frac{\alpha}{\delta+x}\right) \\ y + \beta y\left(1 - \frac{qy}{\gamma+x}\right)\end{pmatrix} \tag{5}$$

The map (5) is considered for the region $\Omega = {\mathbb{R}_+}^2 = \{(x, y) : x \geq 0, y \geq 0\}$.

3 Existence and stability of fixed points

This section illustrates the existence and stability of the fixed points of the map (5).
The fixed points of the map (5) are summarized as follows:

1. The trivial fixed point is $E_0(0, 0)$.
2. The semitrivial fixed points are $E_{x_{1,2}}(x_{1,2}, 0)$, where

$$x_{1,2} = \frac{1}{2}\left(1 - \delta \pm \sqrt{(1-\delta)^2 - 4(\alpha - \delta)}\right),$$

   $\delta < 1$ and $(\delta + 1)^2 > 4\alpha$.
   - If $\alpha > \delta$, then $E_{x_{1,2}}(x_{1,2}, 0)$ both exits provided $(\delta + 1)^2 > 4\alpha$, $\delta < 1$.
   - If $\alpha < \delta$, then E_{x_1} exists only.
3. Another semitrivial fixed points is $E_y(0, \frac{\gamma}{q})$.

4. The positive fixed points are $E_{(xy)_{1,2}} = (x^*_{1,2}, y^*_{1,2})$, where $y^*_{1,2} = \frac{\gamma + x^*_{1,2}}{q}$ and $x^*_{1,2} = \frac{1}{2}\left((1-\delta-\frac{p}{q}) \pm \sqrt{(1-\delta-\frac{p}{q})^2 - 4\delta(\frac{p}{q}+\frac{\alpha}{\delta}-1)}\right)$, where $\frac{p}{q}+\frac{\alpha}{\delta} > 1$.
   - $E_{(xy)_{1,2}}$ both exists, when $\frac{p}{q}+\delta < 1$ and $\left(1-\delta-\frac{p}{q}\right)^2 > 4\delta\left(\frac{p}{q}+\frac{\alpha}{\delta}-1\right)$.
   - If $\left(1-\delta-\frac{p}{q}\right)^2 = 4\delta\left(\frac{p}{q}+\frac{\alpha}{\delta}-1\right)$, then $\bar{E}(\bar{x},\bar{y})$ exists, where $\bar{x} = \frac{1}{2}(1-\delta-\frac{p}{q})$ and $\bar{y} = \frac{\gamma+\bar{x}}{q}$.
   - If $\left(1-\delta-\frac{p}{q}\right)^2 < 4\delta\left(\frac{p}{q}+\frac{\alpha}{\delta}-1\right)$, no positive fixed point exists.

The Jacobian matrix for the discrete map (5) as arbitrary fixed point $(\widehat{x},\widehat{y})$ is given as

$$J(E) = \begin{pmatrix} 2 - \left(2\widehat{x} + \frac{p\gamma\widehat{y}}{(\gamma+\widehat{x})^2} + \frac{\alpha\delta}{(\delta+\widehat{x})^2}\right) & -\frac{p\widehat{x}}{\gamma+\widehat{x}} \\ \frac{q\beta\widehat{y}^2}{(\gamma+\widehat{x})^2} & 1+\beta\left(1-\frac{2q\widehat{y}}{\gamma+\widehat{x}}\right) \end{pmatrix}.$$

The corresponding characteristic equation is written as

$$\lambda^2 - Tr\lambda + Det = 0 \tag{6}$$

where

$$Tr = 3 + \beta - 2\widehat{x} - \frac{p\gamma\widehat{y}}{(\gamma+\widehat{x})^2} - \frac{\alpha\delta}{(\delta+\widehat{x})^2} - \frac{2\beta q\widehat{y}}{\gamma+\widehat{x}}$$
$$Det = \left(2 - 2\widehat{x} - \frac{p\gamma\widehat{y}}{(\gamma+\widehat{x})^2} - \frac{\alpha\delta}{(\delta+\widehat{x})^2}\right)\left(1+\beta-\frac{2\beta q\widehat{y}}{\gamma+\widehat{x}}\right) + \frac{pq\beta\widehat{x}\widehat{y}^2}{(\gamma+\widehat{x})^3}$$

The dynamical behavior of the fixed points can be classified by the following lemma:

Lemma 1. *Consider a polynomial $\tau(\lambda) = \lambda^2 - Tr\lambda + Det$, λ_1 and λ_2 be the eigenvalues. Suppose $\tau(1) > 0$ then*

1. *$|\lambda_1| < 1$ and $|\lambda_2| < 1$ if and only if $\tau(-1) > 0$ and $Det < 1$;*
2. *$|\lambda_1| < 1$ and $|\lambda_2| > 1$ (or $|\lambda_1| > 1$ and $|\lambda_2| < 1$) if and only if $\tau(-1) < 0$;*
3. *$|\lambda_1| > 1$ and $|\lambda_2| > 1$ if and only if $\tau(-1) > 0$ and $Det > 1$;*
4. *$\lambda_1 = -1$ and $\lambda_2 \neq 1$ if and only if $\tau(-1) = 0$ and $Tr \neq 0, 2$;*
5. *λ_1 and λ_2 are complex conjugate and $|\lambda_1| = |\lambda_2|$ if and only if $(Tr)^2 - 4Det < 0$ and $Det = 1$.*

3.1 Dynamical behavior around the trivial fixed point $E_0(0,0)$:

The Jacobian of (5) has eigenvalues $\lambda_1 = 2 - \frac{\alpha}{\delta}$ and $\lambda_2 = 1 + \beta$ at trivial fixed point E_0. The fixed point E_0 is a saddle when $\alpha > \delta$, a source when $\alpha < \delta$ and non-hyperbolic for both conditions $\alpha = \delta$ and $\alpha = 3\delta$.

3.2 Dynamical behavior around the semitrivial fixed points:

(a) The eigenvalues of the Jacobian of the map (5) are $\lambda_1 = 2-2x_{1,2}-\frac{\alpha\delta}{(\delta+x_{1,2})^2}$ and $\lambda_2 = 1+\beta$ at semitrivial fixed point $E_{x_{1,2}}(x_{1,2},0)$. $E_{x_{1,2}}$ is a saddle point if $1 < 2x_{1,2} - \frac{\alpha\delta}{(\delta+x_{1,2})^2} < 3$, a source if $0 \leq 2x_{1,2} - \frac{\alpha\delta}{(\delta+x_{1,2})^2} < 1$ and non-hyperbolic for both the conditions $2x_{1,2} - \frac{\alpha\delta}{(\delta+x_{1,2})^2} = 1$ and $2x_{1,2} - \frac{\alpha\delta}{(\delta+x_{1,2})^2} = 3$.

(b) The eigenvalues are $\lambda_1 = 2 - \frac{p}{q} - \frac{\alpha}{\delta}$ and $\lambda_2 = 1-\beta$ at semitrivial fixed point $E_y(0, \frac{\gamma}{q})$.

3.3 Dynamical behavior at positive fixed point $E_{xy}(x^*, y^*)$:

The characteristic polynomial at $E_{xy}(x^*, y^*)$ is obtained as

$$\tau(\lambda) = \lambda^2 - (3-\beta-A)\,\lambda + (2-A+\beta(B-2))$$

where $A(x^*) = 2x^* + \frac{p\gamma}{q(\gamma+x^*)} + \frac{\alpha\delta}{(\delta+x^*)^2}$ and $B(x^*) = 2x^* + \frac{p}{q} + \frac{\alpha\delta}{(\delta+x^*)^2}$. The stability of the positive fixed point E_{xy} can be discussed by using the following results. The positive fixed point $E_{xy}(x^*, y^*)$ is said to be stable if:

$$\begin{aligned} &Tr(J(E_{xy})) - Det(J(E_{xy})) < 1 \\ &Tr(J(E_{xy})) + Det(J(E_{xy})) > -1 \\ &Det(J(E_{xy})) < 1. \end{aligned} \tag{7}$$

Theorem 1. *The dynamical behavior of the map (5) at positive fixed point $E_{xy}(x^*, y^*)$ is concluded as follows:*

1. *Sink when $\frac{2(A-3)}{B-3} < \beta < \frac{A-1}{B-2}$.*
2. *Source when $\beta > \max\left\{\frac{A-1}{B-2}, \frac{2(A-3)}{B-3}\right\}$ or $\beta < \frac{2(A-3)}{B-3}$.*
3. *Non-hyperbolic if one of the following condition holds:*
   (a) $\beta = \frac{2(A-3)}{B-3}$, $\beta \neq \frac{A-2}{B-2}$ *and* $\beta \neq \frac{A}{B-2}$.
   (b) $\beta = \frac{A-1}{B-2}$ *and* $(1+\beta+A)^2 < 4B\beta + 8$.

4 Bifurcation of codimension 1

This subsection determines the conditions of occurrence of flip bifurcation and Neimark-Sacker bifurcation at positive fixed point $E_{xy}(x^*, y^*)$

Theorem 2. *(i) Flip bifurcation is occurred at $\beta = \frac{2(A-3)}{B-3}$ (ii) Neimark-Sacker bifurcation is occurred at $\beta = \frac{A-1}{B-2}$ around the positive fixed point $E_{xy}(x^*, y^*)$ in map (5).*

Proof.: It is clear, the Jacobian J has eigenvalues $|\lambda_1| \neq 1$ and $\lambda_2 = -1$ at the positive fixed point $E_{xy}(x^*, y^*)$ for $\beta = \frac{2(A-3)}{B-3}$. i.e. E_{xy} is non-hyperbolic.
Let $u = x - x^*$, $v = y - y^*$ and $\mu = \beta - \beta_1$, where $\beta_1 = \frac{2(A-3)}{B-3}$. The fixed

point $E_{xy}(x^*, y^*)$ is shifted to the origin and expanding the right-hand side of map (5), it yields

$$\begin{pmatrix} u \\ v \end{pmatrix} \to \begin{cases} a_{11}u + a_{12}v + a_{13}uv + a_{14}u^2 + a_{15}u^2v + O(|u,v|^4) \\ b_{11}u + b_{12}v + b_{13}\mu + b_{14}v^2 + b_{15}\mu v + b_{16}u^2 + b_{17}\mu u \\ \qquad +b_{18}uv + b_{19}uv^2 + O(|u,v|^4) \end{cases} . \tag{8}$$

where $a_{11} = 2 - 2x^* - \frac{\alpha\delta}{(\delta+x^*)^2} - \frac{p\gamma y^*}{(\gamma+x^*)^2}$, $a_{12} = -\frac{px^*}{\gamma+x^*}$, $a_{13} = -\frac{p\gamma}{(\gamma+x^*)^2}$, $a_{14} = \left(\frac{\alpha\delta}{(\delta+x^*)^3} + \frac{p\gamma y^*}{(\gamma+x^*)^3} - 1\right)$, $a_{15} = \frac{p\gamma}{(\gamma+x^*)^3}$, $b_{11} = \frac{q\beta_1(y^*)^2}{(\gamma+x^*)^2}$, $b_{12} = 1 + \beta_1\left(1 - \frac{2qy^*}{\gamma+x^*}\right)$, $b_{13} = y^*\left(1 - \frac{qy^*}{\gamma+x^*}\right)$, $b_{14} = -\frac{q\beta_1}{\gamma+x^*}$, $b_{15} = \left(1 - \frac{2qy^*}{\gamma+x^*}\right)$, $b_{16} = -\frac{q\beta_1(y^*)^2}{(\gamma+x^*)^3}$, $b_{17} = \frac{q(y^*)^2}{(\gamma+x^*)^2}$, $b_{18} = \frac{2q\beta_1 y^*}{(\gamma+x^*)^2}$ and $b_{19} = -\frac{q\beta_1(y^*)^2}{(\gamma+x^*)^3}$

Now linearizing the map (8) at $(0,0)$ and forming an invertible matrix,

$$T = \begin{pmatrix} \lambda_1 - a_{11} & -a_{11} - 1 & 0 \\ a_{12} & a_{12} & 0 \\ 0 & 0 & 1 \end{pmatrix}.$$

By using the transformation $\begin{pmatrix} u \\ v \\ \mu \end{pmatrix} = T \begin{pmatrix} X \\ Y \\ w \end{pmatrix}$, the map (8) turns into

$$\begin{pmatrix} X \\ Y \\ w \end{pmatrix} \to \begin{pmatrix} \lambda_1 & 0 & 0 \\ 0 & -1 & 0 \\ 0 & 0 & 1 \end{pmatrix} \begin{pmatrix} X \\ Y \\ w \end{pmatrix} + \begin{pmatrix} F_1(X,Y,w) \\ G_1(X,Y,w) \\ 0 \end{pmatrix}$$

where

$$F_1(X,Y,w) = k_1X^2 + k_2Y^2 + k_3XY + k_4X^2Y + k_5XY^2 + k_6X^3 + O(|X,Y|^4)$$
$$G_1(X,Y,w) = e_1Y^2 + e_2wY + k_3wX + e_4XY + e_5X^2 + e_6X^3 + e_7Y^3 + O(|X,Y|^4).$$

Here $k_1 = a_{12}a_{13}(\lambda_1 - a_{11}) + a_{14}(\lambda_1 - a_{11})^2$, $k_2 = a_{14}(1+a_{11})^2 - a_{12}a_{13}(1+a_{11})$, $k_3 = a_{12}a_{13}(\lambda_1 - a_{11}) - a_{12}a_{13}(1+a_{11}) - 2a_{14}(\lambda_1 - a_{11})(1+a_{11})$, $k_4 = a_{15}(\lambda_1 - a_{11})^2 - 2a_{15}(\lambda_1 - a_{11})(1+a_{11})$, $k_5 = 2a_{15}(1+a_{11})^2 - 2(\lambda_1 - a_{11})(1+a_{11})$, $k_6 = a_{15}(\lambda_1 - a_{11})^2$, $e_1 = b_{14} + b_{16}(1+a_{11})^2 - b_{18}(1+a_{11})$, $e_2 = b_{15} - b_{17}(1+a_{11})$, $e_3 = b_{15} + b_{17}(\lambda_1 - a_{11})$, $e_4 = 2b_{14} - 2b_{16}(\lambda_1 - a_{11})(1+a_{11}) + b_{18}(\lambda_1 - a_{11}) - b_{18}(1+a_{11})$, $e_5 = b_{14} + b_{16}(\lambda_1 - a_{11})^2 + b_{18}(\lambda_1 - a_{11})$, $e_6 = a_{12}^2(\lambda_1 - a_{11})$ and $e_7 = -a_{12}^2(1+a_{11})$

To discuss the stability of $(X,Y) = (0,0)$ near $w = 0$, the center manifold is considered as

$$Z^c(0) = \{(X,Y,w) \in R^3 | X = S(Y,w), S(0,0) = 0, DS(0,0) = 0\},$$

here X and w are sufficiently small. Let

$$S(Y,w) = S_1w^2 + S_2wY + S_3Y^2 + O(|Y,w|^3). \tag{9}$$

Then

$$\kappa(S(Y,w),w) = S(-Y + G_1(S(Y,w),Y,w)) - \lambda_1 S(Y,w) - F_1(S(Y,w),Y,w) = 0. \tag{10}$$

Substituting (9) into (10) and comparing the coefficients of (10) we obtain $S_1 = S_2 = 0$ and $S_3 = \frac{k_2}{1-\lambda_1}$.
Then the map (8) restricted to the center manifold is given by

$$Y \sim \widetilde{G_1}(Y,w) = e_1Y^2 - Y + e_2wY + e_3S_3wY^2 + e_4S_3Y^3 + e_5S_3^2Y^4 + e_7Y^3 + O|Y,w|^5$$

It can be seen that $\widetilde{G_1}(0,0) = 0$, $\frac{\partial\widetilde{G_1}}{\partial Y}(0,0) = -1$, $\frac{\partial\widetilde{G_1}}{\partial w}(0,0) = 0$, $\frac{\partial^2\widetilde{G_1}}{\partial Y^2}(0,0) = 2e_1 \neq 0$, $\frac{\partial^2\widetilde{G_1}}{\partial Yw}(0,0) = e_2 \neq 0$ and $\frac{\partial^3\widetilde{F_1}}{\partial Y^3}(0,0) = 6(e_4S_3 + e_7)$.

$$\varrho_1 = \left(\frac{1}{2}\frac{\partial\widetilde{F_1}}{\partial w}\frac{\partial^2\widetilde{F_1}}{\partial X^2} + \frac{\partial^2\widetilde{F_1}}{\partial Xw}\right)$$

$$\varrho_2 = \left(\left(\frac{1}{2}\frac{\partial^2\widetilde{F_1}}{\partial X^2}\right)^2 + \frac{1}{6}\frac{\partial^3\widetilde{F_1}}{\partial X^3}\right)$$

From above equation, $\varrho_1 = e_2 \neq 0$ and $\varrho_2 = e_4S_3 + e_1^2 \neq 0$ (see more details [21,22]).
Therefore, the map (5) occurs flip bifurcation at fixed point E_{xy} for bifurcation parameter $\beta = \frac{2(A-3)}{B-2}$.
(ii) Now, we discuss Neimark-Sacker bifurcation at fixed point E_{xy} is non-hyperbolic at $\beta = \frac{A-1}{B-2}$ for $|\lambda_1| = 1$, $|\lambda_2| = 1$.
We transform the fixed point $E_{xy}(x^*, y^*)$ to the origin and expand the right-hand side of map (5) around the origin by using following translation $u = x - x^*$, $v = y - y^*$ and $\beta_1 = \frac{A-1}{B-2}$. The map (5) yields

$$\begin{pmatrix} u \\ v \end{pmatrix} \rightarrow \begin{cases} a_{11}u + a_{12}v + a_{13}uv + a_{14}u^2 + a_{15}u^2v + O(|u,v|^4) \\ b_{11}u + b_{12}v + b_{13}uv + b_{14}u^2 + b_{15}v^2 + b_{16}u^2v + b_{17}uv^2 + O(|u,v|^4) \end{cases} \tag{11}$$

where $a_{11} = 2 - 2x^* - \frac{\alpha\delta}{(\delta+x^*)^2} - \frac{p\gamma y^*}{(\gamma+x^*)^2}$, $a_{12} = -\frac{px^*}{\gamma+x^*}$, $a_{13} = -\frac{p\gamma}{(\gamma+x^*)^2}$, $a_{14} = \left(\frac{\alpha\delta}{(\delta+x^*)^3} + \frac{p\gamma y^*}{(\gamma+x^*)^3} - 1\right)$, $a_{15} = \frac{p\gamma}{(\gamma+x^*)^3}$, $b_{11} = \frac{q\beta(y^*)^2}{(\gamma+x^*)^2}$, $b_{12} = 1 + \beta\left(1 - \frac{2qy^*}{\gamma+x^*}\right)$, $b_{13} = \frac{2q\beta y^*}{(\gamma+x^*)^2}$, $b_{14} = -\frac{q\beta(y^*)^2}{(\gamma+x^*)^3}$, $b_{15} = -\frac{q\beta}{\gamma+x^*}$, $b_{16} = -\frac{2q\beta y^*}{(\gamma+x^*)^3}$, $b_{17} = \frac{q\beta}{(\gamma+x^*)^2}$.
Let us consider the following set of complex eigenvalues, obtained by linearizing the map (11) at $(0,0)$

$$\lambda_{1,2} = \frac{m(\beta) \pm \iota\sqrt{4n(\beta) - (m(\beta))^2}}{2}$$

with $|\lambda_{1,2}| = \sqrt{n(\beta)}$, followed by the transversality condition

$$\left(\frac{d|\lambda_{1,2}|}{d\beta}\right)_{\beta=\frac{A-1}{B-2}} = \frac{-1}{2\sqrt{n\left(\frac{A-1}{B-2}\right)}} \neq 0.$$

It is required to verify nondegeneracy condition ${\lambda^j}_{1,2} \neq 1, j = 1,2,3,4$ which is equivalent to $m(\beta) \neq 0, -1$ i.e. $A \neq \frac{4}{B-1}$ and $A \neq \frac{B+2}{B-1}$.

Now, assume an invertible matrix

$$T = \begin{bmatrix} a_{12} & 0 \\ M - a_{11} & N \end{bmatrix}$$

$M = \frac{m(\beta)}{2}$, $N = \sqrt{4n(\beta) - (m(\beta))^2}$.
The map (11) becomes

$$\begin{pmatrix} X \\ Y \end{pmatrix} \to \begin{pmatrix} M & -N \\ N & M \end{pmatrix} \begin{pmatrix} X \\ Y \end{pmatrix} + \begin{pmatrix} F_1(X,Y) \\ G_1(X,Y) \end{pmatrix} \tag{12}$$

$$\begin{aligned} F_1(X,Y) &= k_{11}X^2 + K_{22}X^3 + k_{33}XY + k_{44}X^2Y + O(|X,Y|^4) \\ G_1(X,Y) &= e_{11}X^2 + e_{22}Y^2 + e_{33}XY + e_{44}X^2Y + e_{55}X^3 + O(|X,Y|^4), \end{aligned}$$

$k_{11} = a_{12}a_{13}(M - a_{11}) + a_{12}^2 a_{14}$, $k_{22} = a_{12}^2 a_{15}(M - a_{11})$, $k_{33} = -a_{12}a_{13}N$, $k_{44} = -a_{12}^2 a_{15}N$, $e_{11} = a_{12}b_{13}(M - a_{11}) + a_{12}^2 b_{14} + b_{15}(M - a_{11})^2 + a_{12}b_{17}(M - a_{11})^2$, $e_{22} = (b_{15} + a_{12}b_{17})N^2$, $e_{33} = -N(a_{12}b_{13} + 2b_{15}(M - a_{11}) + 2a_{12}b_{17}(M - a_{11}))$, $e_{44} = -a_{12}^2 b_{16}N$ and $e_{55} = b_{16}a_{12}^2(M - a_{11})$.
It is easily noticed that (12) is exactly in form of center manifold, the non-degeneracy condition for the Neimark-Sacker bifurcation is given by

$$\hat{\beta} = -Re\left(\frac{(1-2\lambda)\bar{\lambda}^2}{1-\lambda}\Phi_{11}\Phi_{20}\right) - \frac{1}{2}|\Phi_{11}|^2 - |\Phi_{02}|^2 + Re(\bar{\lambda}\Phi_{21}) \tag{13}$$

where

$$\begin{aligned} \Phi_{20} &= \frac{1}{4}\left[k_{11} + e_{33} + i(e_{11} - e_{22} - k_{33})\right]_{(0,0)} \\ \Phi_{11} &= \frac{1}{2}\left[k_{11} + i(e_{11} + e_{22})\right]_{(0,0)} \\ \Phi_{02} &= \frac{1}{4}\left[k_{11} - e_{33} + i(e_{11} - e_{22} + k_{33})\right]_{(0,0)} \\ \Phi_{21} &= \frac{1}{8}\left[3k_{22} + e_{44} + i(3e_{55} - k_{44})\right]_{(0,0)}. \end{aligned}$$

Thus, the aforementioned argument provides following theorem for the occurrence of Neimark-Sacker bifurcation [21,22]:

Theorem 3. *The map (5) undergoes Neimark-Sacker bifurcation if the both conditions $\beta \neq 3 - A$ and $\beta \neq 4 - A$ holds and $\hat{\beta} \neq 0$ at fixed point E_{xy}. Moreover, if $\hat{\beta} < 0$ ($\hat{\beta} > 0$) then a unique closed invariant curve bifurcates at $\beta = \frac{A-1}{B-2}$ which is supercritical (subcritical) and asymptotically stable (unstable).*

5 Numerical Simulation

In order to substantiate the obtained results and explore the complex dynamics in the map (5), the numerical simulation is performed for the following set of parameters [20]:

$$p = 0.40, \quad q = 1.0, \quad \alpha = 0.10, \quad \gamma = 0.10, \quad \delta = 0.05, \quad \beta = 0.25$$

For these set of parameters, the stability conditions of the fixed point $E_{xy}(x^*, y^*)$ are satisfied. Fig.1 shows the stable dynamics in the system (5). It confirms that both species coexist and converge to fixed point $E_{xy}(0.35, 0.45)$.
For these parameters, the results of first part of theorem 2 holds i.e. $\varrho_1 = -3.13426$, $\varrho_2 = 2741.9$, hence the system (5) undergoes flip bifurcation at E_{xy} and as $\varrho_2 > 0$ which shows period-2 point and its stability. Fig.2 gives bifurcation diagram for the parameter β at $\alpha = 0.095$ (without changing other parameters). The system (5) exhibits flip bifurcation followed by chaos (period doubling route to chaos) at the parameter β. The system shows a stable window upto $\beta = 2.3$, followed by a cascade of period doubling. Further a dense chaotic region is occurred for $\beta \in (2.862, 3.012)$ along with intermittent quasi periodic windows at $(2.94, 2.952)$ which ends to a stable window beyond $\beta = 3.012$. The maximal Lyapunov exponent (MLE) for the same values is plotted in fig.3. The positive value of Lyapunov exponent confirms the presence of chaos in the system.

Further for substantiating the results of theorem 2(ii), we choose the new set of parameters

$$p = 0.9, \quad q = 2.0, \quad \alpha = 0.1695, \quad \gamma = 0.10, \quad \delta = 0.3$$

The value of nondegeneracy condition for Neimark-Sacker bifurcation is $\hat{\beta} = -0.13563 < 0$. According to theorem 3, the fixed point E_{xy} is stable when $\beta < \beta_1$, E^*_{xy} loses its stability and becomes unstable, a closed invariant curve appears when $\beta > \beta_1$. And $\hat{\beta} < 0$, supercritical NSB is occurred. The bifurcation diagram is plotted in (β, x) plane at $\beta_1 = 0.245$ in fig.4, a closed invariant curve appears.

6 Conclusion

In this paper, a discretized form of a modified Leslie-Gower prey-predator model with Michaelis-Menten type harvesting in prey, has been studied. Bifurcation theory and center manifold theory has been employed to exhibit various bifurcations of codimension 1 viz. Neimark-Sacker bifurcation, flip bifurcation. The approximate expression of bifurcation curves is also determined.The numerical simulation gives an extensive presentation about occurrence of different bifurcation and chaos.

References

1. J. B. Collings, The effects of the functional response on the bifurcation behavior of a mite predator–prey interaction model, J. Math. Biol., 36 (1997), 149–168.
2. J. Huang and D. Xiao, Analyses of bifurcations and stability in a predator-prey system with Holling type-IV functional response, Acta Math. Appl. Sinica Eng. Ser., 20 (2004), 167–178.
3. S. Ruan and D. Xiao, Global analysis in a predator-prey system with nonmonotonic functional response, SIAM J. Appl. Math., 61 (2001), 1445–1472.

4. L. Li and Z. J. Wang, Global stability of periodic solutions for a discrete predator–prey system with functional response, Nonlinear Dynam., 72, (2013) 507–516.
5. S. N. Elaydi, Discrete chaos: with applications in science and engineering, Chapman and Hall/CRC, (2007).
6. H. N. Agiza et al., Chaotic dynamics of a discrete prey–predator model with Holling type II, Nonlinear Anal. Real World Appl., 10(2009), 116–129.
7. W. Liu and D. Cai, Bifurcation, chaos analysis and control in a discrete-time predator–prey system, Adv. Difference Equ., Springer, 2019.
8. E. M. Elabbasy, A. A. Elsadany and Y. Zhang, Bifurcation analysis and chaos in a discrete reduced Lorenz system, Appl. Math. Comput., 228(2014), 184–194.
9. Q. Din, Complexity and chaos control in a discrete-time prey-predator model, Commun. Nonlinear Sci. Numer. Simul., 49(2017), 113–134.
10. A. Singh, A. A. Elsadany and A. Elsonbaty, Complex dynamics of a discrete fractional–order Leslie–Gower predator–prey model, Math. Methods Appl. Sci., 42(2019), 3992–4007.
11. A. Singh and P. Deolia, Dynamical analysis and chaos control in discrete-time prey-predator model, Commun. Nonlinear Sci. Numer. Simul., 90(2020), 105313.
12. J.M. Smith, Mathematical Ideas in Biology, Cambridge University Press, Cambridge, (1968).
13. S. H. Levine, Discrete time modeling of ecosystems with applications in environmental enrichment, Math. Biosci., 24(1975), 307–317.
14. X. Liu and D. Xiao, Bifurcations in a discrete time Lotka-Volterra predator-prey system, Discrete Contin. Dyn. Syst. Ser. B, 69 (2006), 559–572.
15. K. P. Hadeler and I. Gerstmann, The discrete Rosenzweig model, Math. Biosci., 98(1990), 49–72.
16. S. Li and W. Zhang, Bifurcations of a discrete prey-predator model with Holling type II functional response, Discrete Contin. Dyn. Syst. Ser B, 14 (2010), 159–176.
17. M. A. Aziz-Alaoui and M. Daher Okiye, Boundedness and global stability for a predator-prey model with modified Leslie-Gower and Holling-Type II schemes, Appl. Math. Lett., 16(2003), 1069–1075.
18. C. Ji, D. Jiang and N. Shi, Analysis of a predator-prey model with modified Leslie-Gower and Holling-type II schemes with stochastic perturbation, J. Math. Anal. Appl., 359(2009), 482–498.
19. C. Ji, D. Jiang and N. Shi, A note on a predator-prey model with modified Leslie-Gower and Holling-type II schemes with stochastic perturbation, J. Math. Anal. Appl., 377(2011), 435–440.
20. R. P. Gupta and P. Chandra, Bifurcation analysis of modified Leslie-Gower predator-prey model with Michaelis-Menten type prey harvesting, J. Math. Anal. Appl., 398 (2013), 278–295.
21. Y, Kuznetsov, Elements of Applied Bifurcation Theory, Springer-Verlag, New York, (1998).
22. J. Huang et al., Bifurcations in a discrete predator–prey model with nonmonotonic functional response, J. Math. Anal. Appl., 464(2018), 201–230.

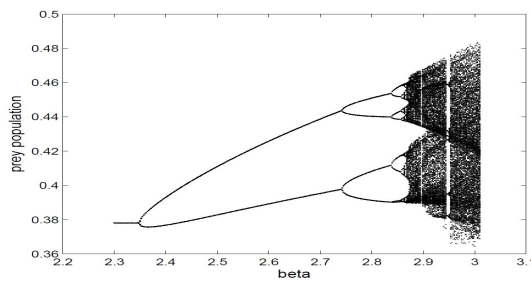

Fig. 1. Bifurcation diagram w. r. to β

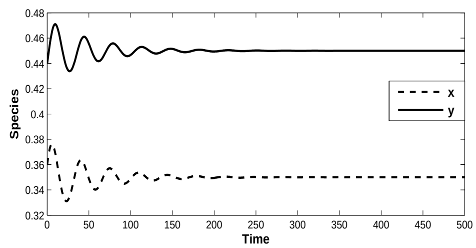

Fig. 2. Stable time series at $\beta = 0.25$

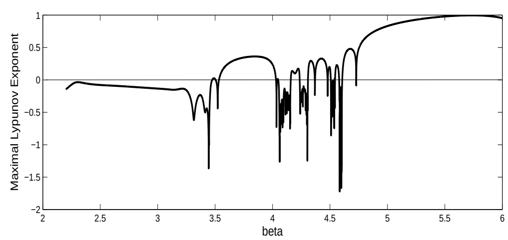

Fig. 3. Maximal Lyaupnov exponent w. r. to β

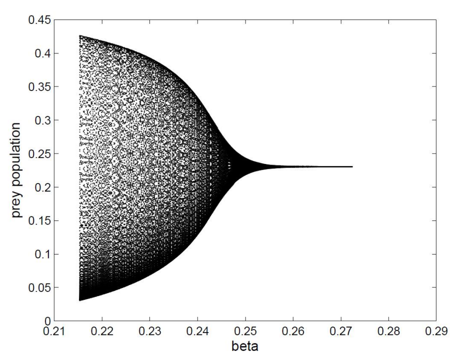

Fig. 4. NSB diagram w. r. to β